

# Catalytic Conversion of Waste Particle Board to Bio-Oil Using Nanoporous Catalyst

Young-Kwon Park<sup>1,2,\*</sup>, Suek Joo Choi<sup>2</sup>, Jong-Ki Jeon<sup>3</sup>, Sung Hoon Park<sup>4</sup>, Ryong Ryoo<sup>5</sup>, Jeongnam Kim<sup>5</sup>, and Kwang-Eun Jeong<sup>6,\*</sup>

<sup>1</sup>School of Environmental Engineering, University of Seoul, Seoul 130-743, Republic of Korea

<sup>2</sup>Graduate School of Energy and Environmental System Engineering, University of Seoul, Seoul 130-743, Republic of Korea

<sup>3</sup>Department of Chemical Engineering, Kongju National University, Cheonan 331-717, Republic of Korea

<sup>4</sup>Department of Environmental Engineering, Sunchon National University, Suncheon 540-742, Republic of Korea

<sup>5</sup>Department of Chemistry, and Graduate School of Nanoscience and Nanotechnology (WCU), KAIST, Daejeon 305-701, Republic of Korea

<sup>6</sup>Green Chemistry Process Research Division, Korea Research Institute of Chemical Technology, Daejeon 305-600, Republic of Korea

The catalytic pyrolysis of waste wood including the particle board was examined by pyrolysis gas chromatography/mass spectrometry (Py-GC/MS) to produce bio-oil. Three different catalysts with a nanoporous structure, Al-MCM-48, Meso-MFI, and Pt-Meso-MFI, were used and their performances were compared. When MCM-48 was used, the quality of the bio-oil product was better than that prepared by non-catalytic pyrolysis but the improvement was limited due to its weak acid sites. On the other hand, Meso-MFI, which has both an MFI structure and strong acid sites, exhibited much better cracking ability and higher selectivity for aromatics. Moreover, Pt-impregnation on Meso-MFI resulted in an even higher selectivity for aromatics and phenolics, which are important raw materials in various petroleum chemical processes.

**Keywords:** Catalytic Pyrolysis, Py-GC/MS, Waste Particle Board, Al-MCM-48, Meso-MFI, Pt-Meso-MFI.

## 1. INTRODUCTION

Renewable energy is attracting increasing attention from researchers all over the world due to global warming and the depletion of fossil fuels. Renewable energy sources that can replace the conventional fossil fuels and nuclear energy include solar energy, bio-energy, wind, tidal power and waste. Among these, waste has a huge energy potential, accounting for approximately 62.6% of the current renewable energy use in South Korea. Waste biomass, (e.g., wood chips, particle boards, and MDF), can pollute the surrounding water system and soil if left untreated. Therefore, utilizing waste biomass is important in terms of energy supply and environment conservation.

Among the many methods for obtaining bio-energy from waste biomass, the thermochemical method, including gasification, combustion and pyrolysis, is the best way of producing bio-energy from large amounts of biomass.<sup>1–5</sup> In particular, pyrolysis is aimed at producing liquid fuel

called *bio-oil*. Compared to fossil fuels, however, the quality of bio-oil as a fuel is low in terms of stability and heating value because of its high oxygen content. Therefore, considerable effort has been made in the catalytic upgrading of bio-oil.<sup>6–12</sup> Hydrogenation and cracking processes are the two most representative catalytic upgrading methods. Hydrogenation, in which bio-oil is upgraded by supplying a large amount of hydrogen gas at a high pressure, is expensive. On the other hand, the cracking process, which uses acid catalysts, such as zeolites, can be performed under atmospheric pressure without a hydrogen supply, making it more economical. Among the acid catalysts, ZSM-5 is particularly efficient for bio-oil upgrading because it not only has high activity for deoxygenation and aromatization but it also suppresses the formation of coke. Nevertheless, one drawback of ZSM-5 is that it contains only micropores, which is disadvantageous in decomposing bio-oil composed of large molecules. Nanoporous catalysts, such as MCM-48, whose pore size is >2 nm, allow large bio-oil molecules to diffuse through the pore structure due to their large pore size.<sup>13</sup>

\*Authors to whom correspondence should be addressed.

Nevertheless, nanoporous catalysts have relatively weak acid sites compared to ZSM-5. This was the motivation for the development of the new catalyst Meso-MFI, which has both strong acid sites and nanopores.<sup>8,14</sup> Catalytic pyrolysis has been studied extensively using a range of biomass materials including raw wood, but there are few reports on the catalytic pyrolysis of waste wood.

Py-GC/MS is a very effective method for directly analyzing the pyrolysis products. In particular, it can determine the relationship between the catalyst properties and products. In the present study, the pyrolysis of waste particle boards was carried out using Py-GC/MS and nanoporous catalysts for the first time. The effect of temperature on the pyrolysis products was examined. Three nanoporous catalysts, Al-MCM-48, Meso-MFI and Pt-Meso-MFI, were applied to the pyrolysis of waste particle boards.

## 2. EXPERIMENTAL DETAILS

### 2.1. Particle Board Sample

The samples were analyzed using an elemental analyzer (Flash EA 1112 series/CE Instruments). The C, H, N and S contents were measured at 1,100 °C and the O content was measured at 1,060 °C under reducing conditions.

Proximate analysis was carried out to measure the moisture, volatile matter, ash and fixed carbon content. The ASTM D2016-74, ASTM E897-82, and ASTM D1102-84 standards were used to measure the moisture, volatile matter and ash, respectively. An approximately 4 mg sample was heated from ambient temperature to 110 °C in a nitrogen-atmosphere and was examined using thermal gravimetric analyzer (TGA, Perkin Elmer-pyris 1). The sample was left at 110 °C for 1 h to measure the moisture content after which it was heated to 900 °C to measure the volatile content. The sample was then placed in an oxygen atmosphere at 800 °C until there was no longer any change in the sample mass to measure the fixed carbon content. The residue was considered to be ash. The analyses results are listed in Table I.

### 2.2. Synthesis of Catalyst

MCM-48 and Meso-MFI catalysts were synthesized using the method described elsewhere.<sup>9,15,16</sup> Al-MCM-48 was

impregnated using the post-synthetic grafting method. Pt-Meso-MFI was synthesized by ion-exchanging the Meso-MFI material with 0.5 wt% Pt(NH<sub>3</sub>)<sub>4</sub>(NO<sub>3</sub>)<sub>2</sub> and calcining it at 500 °C for 3 h.

### 2.3. Py-GC/MS Analysis

The vapor-phase products, which had been catalytically upgraded indirectly using a single-shot pyrolyzer (Frontier-Lab Co., Py-2020iD), were introduced into a GC/MS. Three different pyrolysis temperatures were used: 350, 450 and 550 °C. Biomass (1 mg) was placed on the sample cup floor above which an intermediate layer of quartz wool was located. Catalyst (1 mg) was installed above the quartz wool layer so that the vapor-phase pyrolysis products could be upgraded while passing the catalyst. A metal capillary column (Ultra ALLOY-5MS/HT; 5% diphenyl and 95% dimethylpolysiloxane, length 30 m, i.d. 0.25 mm, film thickness 0.5 μm, Frontier Laboratories Ltd. Japan) was used for analysis. The experiments were repeated at least three times. The product composition is reported as the peak area%. For more details regarding the analysis method, please refer to “Bae et al.”<sup>17</sup>

## 3. RESULTS AND DISCUSSION

### 3.1. Catalyst Characterization

Table II lists the Si/Al ratios and specific surface area properties of the catalysts used in this study. Al-MCM-48 had a larger specific surface area than Meso-MFI. Pt-Meso-MFI had a smaller specific surface area than Meso-MFI due to the decrease in surface area from the addition of Pt.

Figure 1 shows the XRD patterns of the nanoporous catalysts. The results were in good agreement with those reported in the literature for all the catalysts tested, indicating that the catalysts had been synthesized properly.

Figure 2 shows the NH<sub>3</sub>-TPD results of the catalysts. Meso-MFI contains a larger amount of acid sites than Al-MCM-48. In addition, most acid sites of Al-MCM-48 are weak acid sites appearing at approximately 250 °C, whereas Meso-MFI contains a considerable amount of strong acid sites appearing at approximately 400 °C. When Pt was added (Pt-Meso-MFI), the amount of strong acid sites was reduced because they were ion-exchanged with Pt, but it was still considerably higher than the amount of strong acid sites of Al-MCM-48. While Al-MCM-48

**Table I.** Ultimate and proximate analyses of the particle board.

Ultimate analysis (wt%)	Proximate analysis (wt%)		
C	44.4	Moisture	2.6
H	5.1	Volatile matters	79.4
O	48.9	Fixed carbon	15.9
N	1.6	Ash	2.1
S	—		

**Table II.** Physical properties of the catalysts.

	S <sub>BET</sub> (m <sup>2</sup> /g)	V <sub>tot</sub> (cm <sup>3</sup> /g)	Average pore size (nm)
Al-MCM-48	1350	1.21	2.6
Meso-MFI	567	0.7	4.1
Pt-Meso-MFI	486	0.7	4.2

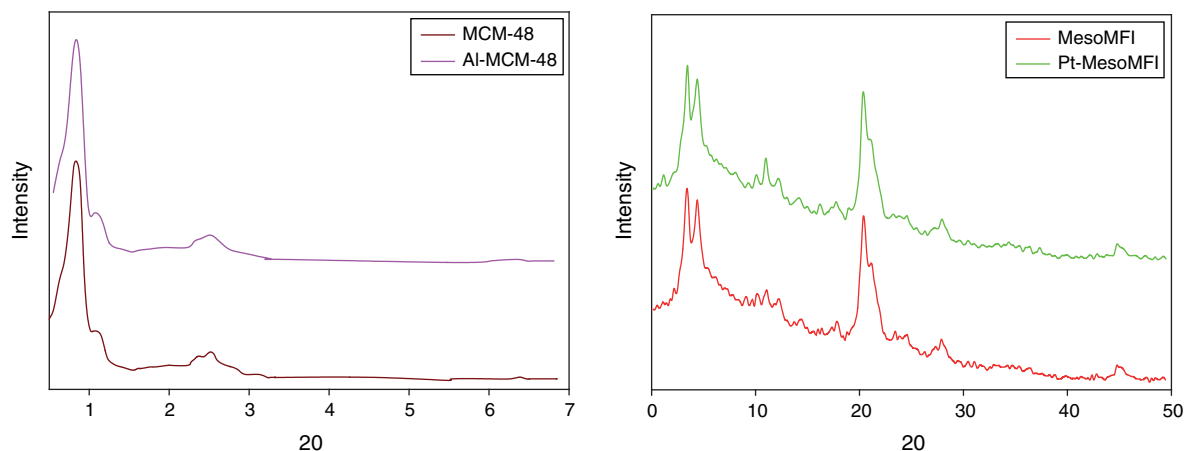


**Fig. 1.** XRD patterns of the nanoporous catalysts.

has mostly weak Lewis acid sites, Meso-MFI and Pt-Meso-MFI have both Lewis acid sites and Brønsted acid sites.<sup>18,19</sup> Since strong acid sites play an important role in the cracking reaction of bio-oil, the two Meso-MFI catalysts were expected to exhibit higher activities in cracking the pyrolysis products than Al-MCM-48.

### 3.2. Thermogravimetric Analysis (TGA)

TGA was carried out to determine the minimum reaction temperature for the pyrolysis experiments and to examine the thermogravimetric properties of the biomass material. Figure 3 shows the TGA result. Approximately 4 mg of biomass was used as the sample. Nitrogen gas with a flow rate of 60 ml/min was used as the carrier gas. The sample was heated to 800 °C with a temperature rising rate of 25 °C/min. Decomposition of the biomass began at approximately 200 °C and was almost complete at approximately 420 °C. The mass reduction occurring at approximately 100 °C was attributed to evaporation of moisture from the biomass. The two DTG peaks appearing

at approximately 320 °C and between 320 and 420 °C were assigned mainly to the decomposition of hemicellulose and cellulose, respectively. The difference in the decomposition temperatures of hemicellulose and cellulose can be explained by the difference in their molecular structures. Cellulose is a homogeneous polysaccharide consisting of only one type of unit molecule, D-glucopyranose. Therefore, the intramolecular bonds within a cellulose polymer form a uniform crystal structure. On the other hand, hemicellulose is a heterogeneous polysaccharide consisting of a range of hexoses and pentoses, with low intramolecular bond strength and a low degree of polymerization compared to cellulose. The mass reduction above 420 °C was attributed to the decomposition of lignin, which decomposes slowly at high temperatures due to its very complex molecular structure. Based on the TGA result, the pyrolysis experiments were carried out at temperatures ranging from 350 to 550 °C.

### 3.3. Pyrolysis of Particle Board Using Py-GC/MS

#### 3.3.1. Noncatalytic Thermal Pyrolysis

The pyrolysis products obtained at 350, 450 and 550 °C using Py-GC/MS were divided into six groups: acids, oxygenates, aromatics, high-hydrocarbons, phenolics, and *N*-compounds. Figure 4 shows the contents of these groups expressed as the area%. The acid and oxygenate contents decreased with increasing temperature due to the enhanced cracking of these species, whereas the phenolics content increased with temperature. This was attributed to the decomposition of lignin. Generally, an increase in reaction temperature appears to result in enhanced deoxygenation reactions due to the thermal catalytic effect.

Higher hydrocarbons ( $C_{20}$  or larger) were not cracked even above 550 °C. The aromatic content, which is a high value-added product, slightly increased with temperature.

Figure 5 shows the content of each oxygenate species. With increasing temperature, cracking of polymer lignin

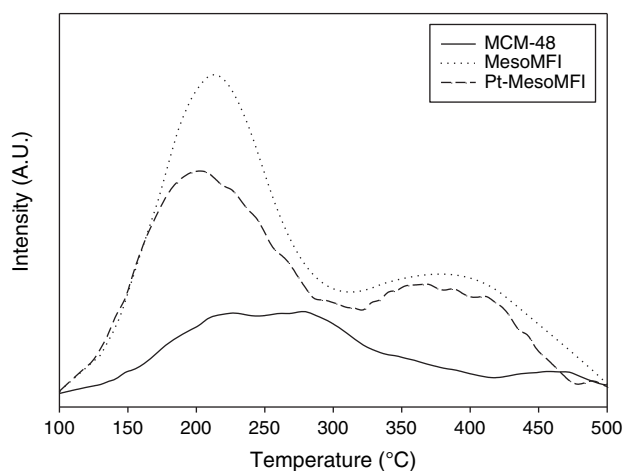


**Fig. 2.**  $NH_3$  TPD of the nanoporous catalysts.

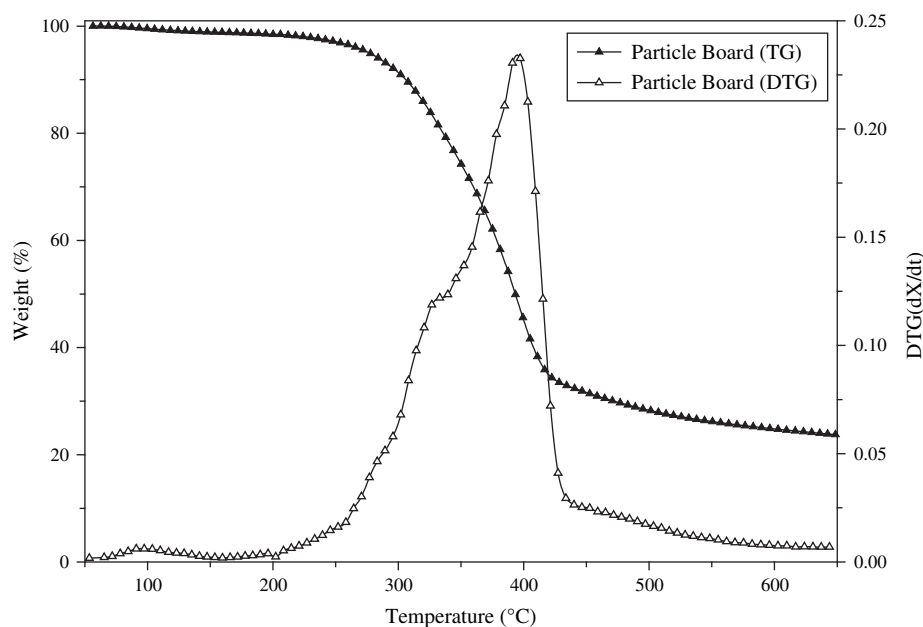


Fig. 3. TG and DTG curves of the particle board with a heating rate of 25 °C/min.

species levoglucosan was enhanced, resulting in the increased production of low-molecular-mass species, such as furans, furanones and cyclopentenones. The contents of aldehydes, esters and carboxylates (the other oxygenates in Fig. 5), which degrade the quality of the product oil, decreased with increasing temperature due to enhanced cracking. The cracking of oxygenates by deoxygenation reactions might result in the production of phenolics, as indicated by the good correlation between the decrease in oxygenates and increase in phenolics, as shown in Figure 4.

Figure 6 presents the contents of phenolic compounds obtained at different temperatures. Hydroxy-phenyl, guaiacyl-phenyl, and syringyl-phenyl are the

main phenyl groups comprising lignin. The content of phenolic compounds generally increased with temperature.

### 3.3.2. Catalytic Pyrolysis

Figure 7 presents the pyrolysis product distributions obtained at 450 °C using different catalysts. The product distributions obtained by noncatalytic thermal pyrolysis were compared. The acid content was decreased by the catalytic upgrading. Also, considerable decreases by catalytic upgrading occurred for the higher hydrocarbons and oxygenates. In particular, Meso-MFI and Pt-Meso-MFI were quite effective in converting higher hydrocarbons and oxygenates into other species, probably due to their strong acid sites. Al-MCM-48 exhibited a lower catalytic activity than Meso-MFI because it contains fewer strong acid

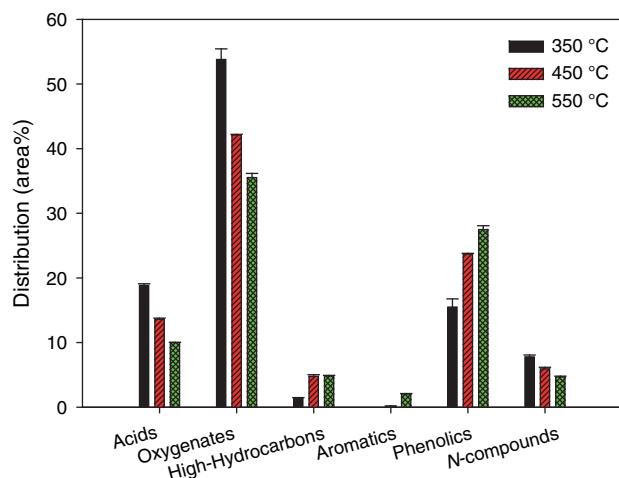


Fig. 4. Product distributions obtained from the pyrolysis of the waste particle board at different temperatures.

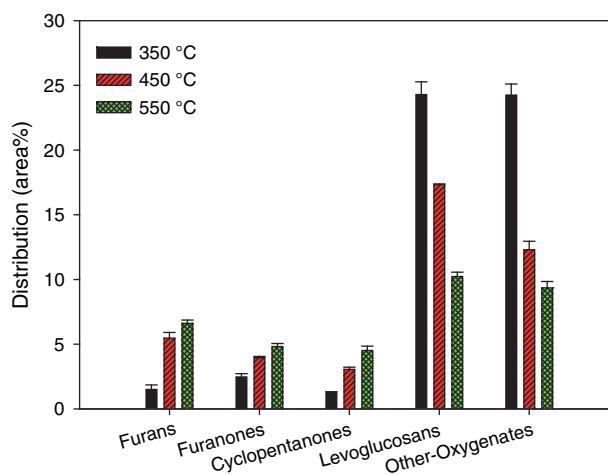
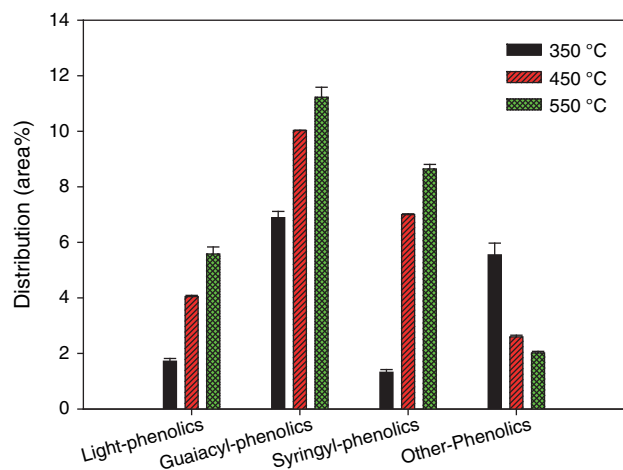


Fig. 5. Effect of temperature on the conversion of the oxygenates.



**Fig. 6.** Effect of temperature on the phenolics.

sites. Pt-Meso-MFI showed higher activity than Meso-MFI despite its smaller specific surface area because of the hydrogenolysis function of Pt: hydrogen produced during the bio-oil upgrading reactions causes a hydrogenolysis reaction, which leads to an enhanced upgrading reaction over the Pt-Meso-MFI catalyst. The phenolic content considerably increased by catalytic upgrading. Meso-MFI showed much better selectivity for the aromatics than MCM-48, which was attributed to its strong acid sites as well as from the shape selectivity related to the MFI structure.<sup>18</sup> When Pt was added, the aromatic content increased further. Pt-Meso-MFI promotes the dehydrogenation reaction producing more alkenes, which can be converted to aromatics on the strong Brönsted acid sites.<sup>8, 18</sup>

Figure 8 shows the content of oxygenate species after catalytic pyrolysis. Polymer oxygenates, such as levoglucosan, were all cracked and not detected when catalytic upgrading was conducted. The cracked polymer

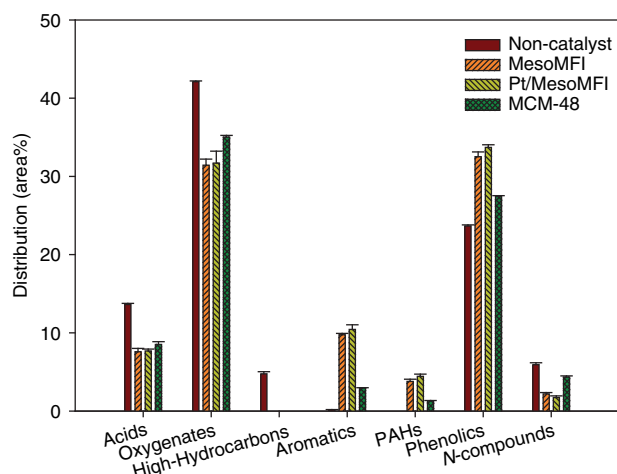


**Fig. 7.** Product distributions obtained from the catalytic pyrolysis of the waste particle board at 450 °C.

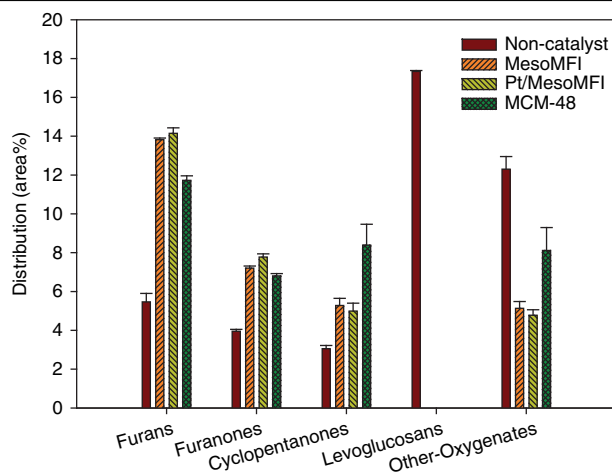


**Fig. 8.** Effect of the catalyst on the product distribution of the oxygenates.

oxygenates are believed to have been converted to low-molecular-mass species, such as furans and cyclopentanones. Aldehydes, esters and carboxylates (the other oxygenates in Fig. 8), which degrade the bio-oil quality, were also cracked by catalytic upgrading. Meso-MFI showed a more remarkable effect on the reduction of oxygenates than MCM-48 because Meso-MFI contains more strong Brönsted acid sites, which are required for cracking and deoxygenation than MCM-48.

Figure 9 shows the results for the phenolics after catalytic pyrolysis. Lignin is composed of hydroxyl-phenyl, guaiacyl-phenyl and syringyl-phenyl forming a chain structure. Hydroxyl-phenol, guaiacyl-phenol, and syringyl-phenol are produced when lignin is cracked upon catalytic upgrading. The use of Meso-MFI resulted in larger increases in light-phenol, guaiacyl-phenol, and syringyl-phenol production than MCM-48 because the strong acid sites of Meso-MFI lead to the more enhanced cracking of lignin. The increase in phenolics species

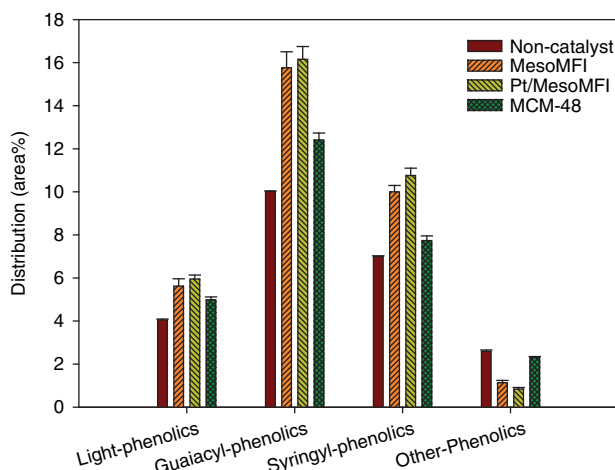


**Fig. 9.** Effect of the catalyst on the product distribution of the phenolics.

obtained with Pt-addition is believed to be due to the additional cracking ability of Pt.<sup>18</sup>

#### 4. CONCLUSIONS

The pyrolysis of particle board using Py-GC/MS showed that bio-oil is composed mainly of oxygenates, phenolics and acids, with smaller amounts of aromatics and hydrocarbons. With increasing pyrolysis temperature, the level of oxygenates decreased and the content of phenolics and high-value-added aromatics increased.

When catalytic upgrading was applied, the oxygenates were removed by catalytic cracking resulting in bio-oil with a higher heating value and better quality. MCM-48 showed poorer performance in catalytic cracking than Meso-MFI because it contains only weak acid sites. Meso-MFI, which has both an MFI structure and strong acid sites, exhibited superior cracking ability and high selectivity for aromatics. The aromatic and phenolic contents in bio-oil were increased when Pt was added to Meso-MFI.

**Acknowledgments:** This research was supported by Basic Science Research Program through the National Research Foundation of Korea (NRF) funded by the Ministry of Education, Science and Technology (No. 2009-0072328). Ryong Ryoo and Jeongnam Kim acknowledge supports from the National Honor Scientist Program (20100029665) and the World Class University Program (R31-2010-000-10071-0) of the Ministry of Education, Science and Technology in Korea.

#### References and Notes

1. H. S. Heo, S. G. Kim, K. E. Jeong, J. K. Jeon, S. H. Park, J. M. Kim, S. S. Kim, and Y. K. Park, *Bioresour. Technol.* 102, 3952 (2011).
2. J. W. Kim, S. H. Lee, S. S. Kim, S. H. Park, J. K. Jeon, and Y. K. Park, *Korean J. Chem. Eng.* 28, 1867 (2011).
3. H. S. Heo, H. J. Park, J. I. Dong, S. H. Park, S. Kim, D. J. Suh, Y. W. Suh, S. S. Kim, and Y. K. Park, *J. Ind. Eng. Chem.* 16, 27 (2010).
4. H. S. Heo, H. J. Park, J. H. Yim, J. M. Sohn, J. Park, S. S. Kim, C. Ryu, J. K. Jeon, and Y. K. Park, *Bioresour. Technol.* 101, 3672 (2010).
5. Y. M. Kim, H. W. Lee, S. H. Lee, S. S. Kim, S. H. Park, J. K. Jeon, S. Kim, and Y. K. Park, *Korean J. Chem. Eng.* 28, 2012 (2011).
6. H. J. Park, H. S. Heo, J. H. Yim, J. K. Jeon, Y. S. Ko, S. S. Kim, and Y. K. Park, *Korean J. Chem. Eng.* 27, 73 (2010).
7. H. J. Park, J. K. Jeon, D. J. Suh, Y. W. Suh, H. S. Heo, and Y. K. Park, *Catal. Surv. Asia.* 15, 161 (2011).
8. H. J. Park, H. S. Heo, J. K. Jeon, J. Kim, R. Ryoo, K. E. Jeong, and Y. K. Park, *Appl. Catal. B: Environ.* 95, 365 (2010).
9. S. H. Lee, H. S. Heo, K. E. Jeong, J. H. Yim, J. K. Jeon, K. Y. Jung, Y. S. Ko, S. S. Kim, and Y. K. Park, *J. Nanosci. Nanotechnol.* 11, 759 (2011).
10. Y. K. Park, H. Y. Lee, J. K. Jeon, S. S. Kim, C. Ryu, J. M. Kim, H. J. Chae, and K. E. Jeong, *Res. Chem. Intermed.* 37, 1283 (2011).
11. S. S. Kim, S. H. Park, J. K. Jeon, D. Chang, S. C. Kim, K. H. Lee, and Y. K. Park, *Res. Chem. Intermed.* 37, 1355 (2011).
12. M. J. Jeon, S. S. Kim, J. K. Jeon, S. H. Park, J. M. Kim, J. M. Sohn, S. H. Lee, and Y. K. Park, *Nanoscale Res. Lett.* 7, 18 (2012).
13. H. W. Lee, H. J. Cho, J. H. Yim, J. M. Kim, J. K. Jeon, J. M. Sohn, K. S. Yoo, and Y. K. Park, *J. Ind. Eng. Chem.* 17, 504 (2011).
14. K. H. Park, H. J. Park, J. Kim, R. Ryu, J. K. Jeon, J. Park, and Y. K. Park, *J. Nanosci. Nanotechnol.* 10, 355 (2010).
15. H. W. Lee, J. K. Jeon, S. H. Park, K. E. Jeong, H. J. Chae, and Y. K. Park, *Nanoscale Res. Lett.* 6, 500 (2011).
16. S. S. Kim, H. S. Heo, S. G. Kim, R. Ryoo, J. Kim, J. K. Jeon, S. H. Park, and Y. K. Park, *J. Nanosci. Nanotechnol.* 11, 6167 (2011).
17. Y. J. Bae, C. Ryu, J. K. Jeon, J. Park, D. J. Suh, Y. W. Suh, D. Chang, and Y. K. Park, *Bioresour. Technol.* 102, 3512 (2011).
18. H. J. Park, K. H. Park, J. K. Jeon, J. Kim, R. Ryoo, K. E. Jeong, S. H. Park, and Y. K. Park, *Fuel* 97, 379 (2012).
19. N. You, J. H. Yim, S. J. Lee, J. H. Lee, Y. K. Park, and J. K. Jeon, *J. Nanosci. Nanotechnol.* 7, 3800 (2007).

Received: 2 August 2011. Accepted: 12 January 2012.